

A Comparison of Neutron and High Energy Synchrotron Radiation as Tools for Texture and Stress Analysis

A. Pyzalla¹, W. Reimers¹ and K.-D. Liss²

¹Strukturforschung, Hahn-Meitner-Institut Berlin GmbH, Glienickerstr. 100,
DE-14109 Berlin, Germany

²European Synchrotron Radiation Facility ESRF, BP 220, FR-38043 Grenoble Cedex, France

Keywords: Neutron Diffraction, Residual Stress, Stress Gradients, Synchrotron Radiation, Texture

Abstract

The experimental set-up for experiments using high energy synchrotron radiation for residual stress analysis is described. The implications of the measurement parameters and the material are discussed. The method is compared to neutron diffraction.

1. Introduction

A non-destructive residual stress analysis can be performed using diffraction methods. Due to the low penetration depth of the characteristic X-rays in technical, especially metallic materials, only the strain and stress distribution in the near surface layers are accessible. An increase in information depth can be achieved using neutron diffraction [1]. Due to the comparatively low neutron flux the local resolution is in the order of a gauge volume size of approximately 1 mm³. The dimension of the gauge volume could be reduced significantly by using high energy monochromatic synchrotron radiation [2].

An alternative to the use of the monochromatic radiation is the use of a white beam in an energy dispersive arrangement [3,4], which gives access to an even higher energy range than the monochromatic radiation. White synchrotron radiation was employed for strain [5,6] and recently white high energy synchrotron radiation was used for stress analyses [7] on a variety of different materials and problems. Those experiments revealed that residual stress analyses using high energy synchrotron radiation with a local resolution of some ten micrometers are possible. Here, the advantages as well as the limits of this method compared to neutron diffraction will be discussed.

2. Basic principle of residual stress analysis by energy dispersive diffraction

From the energy dispersive spectrum the line position of a large number of reflections can be obtained by fitting the reflection profile using a suitable e.g. a Gauss distribution. The energy value E^{hkl} representing the line position corresponds to the lattice spacing d^{hkl} including the lattice strain. The lattice spacing d^{hkl} and the strain ϵ_i^{hkl} can be calculated from the respective energy value according to Bragg's law

$$d^{hkl} = \frac{hc}{2 \sin \theta E^{hkl}} = \text{const.} \cdot \frac{1}{E^{hkl}}, \quad \epsilon_i^{hkl} = \frac{d_i^{hkl} - d_0^{hkl}}{d_0^{hkl}} = \frac{E_0}{E_i^{hkl}} - 1$$

with hkl denoting Miller's indices, θ is the Bragg angle, h is Planck's constant and c is the velocity of light. The residual stresses then can be calculated using Hooke's law.

3. Set-up of the experiment

The set-up for an experiment for residual stress analysis by energy dispersive synchrotron radiation is illustrated in fig. 1 using the example of the modified triple axis diffractometer at the High Energy Diffraction Beam Line (ID15A) at the European Synchrotron Radiation Facility (ESRF) Grenoble, France.

The spectral range in case of the asymmetric wiggler as an insertion device has a broad maximum with a peak brightness of $3.3 \cdot 10^{14}$ $\frac{\text{photons}}{\text{s mrad}^2}$, 0.1% bw, 100mA

at 50 keV. The beam has a horizontal divergence of $\Delta\theta_0^h \cong 1.27 \cdot 10^{-3}$ and a vertical divergence of $\Delta\theta_0^v \cong 1 \cdot 10^{-4}$ [8]. A horizontal slit can be mounted in the optics hutch, which has a distance of several m (here 3.5 m) to the sample position. After trespassing the slit the beam is diffracted within the sample and again passes two slits. Then the energy spectrum is analysed in a Ge semiconductor detector.

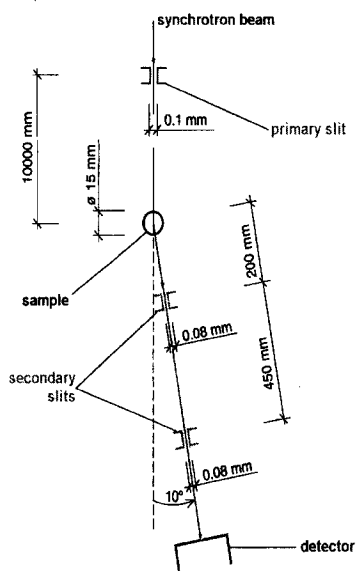


Fig. 1: Experimental set-up at the high energy beamline ID 15A at the ESRF

4. Penetration depth of the high energy synchrotron radiation

Major criterions for the feasibility of residual stress analyses using a certain radiation are the intensity of the reflections and the penetration depth of the beam. In fig. 2 the 50 % transmission thickness for synchrotron radiation in case of the four major construction materials, tungsten and a ZrO₂ ceramic are shown. Due to the decrease of the attenuation coefficient with increasing energy of the radiation [9], in case of high energies the 50 % transmission thickness increases to app. 2 mm at 100 keV in Fe (neutrons: 5,8 mm [10]) and Ni (neutrons: 3,9 mm [10]) and even up to 15 mm in Al (neutrons: 69,3 mm [10]). Due to the photon flux at the beamline ID 15 A of the ESRF Grenoble ($1,6 \cdot 10^{13}$ photons / (s cm² 0.1% bw., 200 mA), at the sample position), which is about 6 orders of magnitudes higher than the neutron flux (10^7 neutrons/ cm² s) at the sample

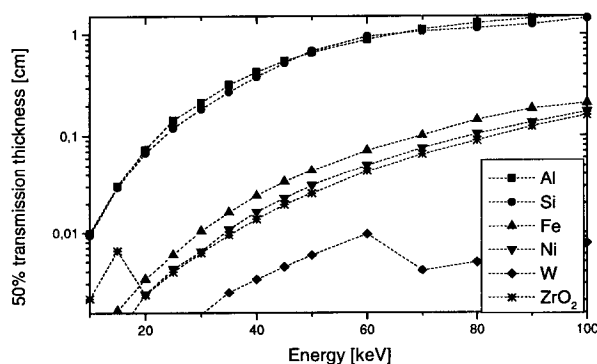


Fig. 2 Dependence of the 50% transmission thickness of the sample material on the energy

position) at a typical residual stress instrument at a reactor source, residual stress analysis on small volume elements (app. 0.1 mm³ in case of high energy synchrotron radiation compared to ca. 1 mm³ in case of neutrons) is often significantly shorter measuring times than in case of neutron diffraction can be performed.

5. Measurement Parameters

Shape of the Volume Element

The shape and the extensions of the gauge volume and thus the volume element studied depend on the gaps d_p of the primary res. d_s the secondary slits, the distance L_1 respectively L_2 of the slits to the sample, the divergence of the beam primary to the sample δ_p and δ_s after trespassing the sample as well as on the Bragg angle θ chosen (Fig. 3).

While in neutron diffraction the 90° scattering technique often permits the use of nearly cubic volume elements, due to the rather small Bragg angle θ in transmission geometry the volume element's shape can be described approximately as an elongated diamond that is significantly longer than wide. A typical volume element size at ID15a at the ESRF is $80\mu\text{m} \times 1650\mu\text{m} \times \text{height}$ (variable). The small width of the volume element obtainable allows for residual stress analyses with a high local resolution in at least one direction. The exact width and length as well as the asymmetry of the volume element can be calculated e.g. by describing its boundaries by appropriate curves and their points of intersection [11]. However, the width B_V and the length L_V of the volume element also can be estimated with an accuracy of some μm as

$$B_V \equiv d_p + 2L_1 \tan(\delta_p), \quad L_V \equiv \frac{B_V}{\tan \theta}$$

in those cases where the distance of the primary slit d_p and the secondary slit d_s as well as the divergence primary to the sample δ_p and after the sample δ_s are in the same order of magnitude and the distance of the secondary slit to the sample is small. If a sharp definition of the volume element's shape is required the secondary slit should be positioned as near to the sample as possible although due to the small divergence of the synchrotron beam this is not as crucial as it has been found in case of neutron diffraction [12]. With respect to the diffraction angle 2θ the ratio of length to width of the volume element steeply increases with decreasing 2θ (fig. 3).

Intensity of the Reflections

Fig. 3 reveals that due to the decrease of the form factor, the intensity of the reflections in the high energy spectrum decreases steeply with increasing 2θ . Thus, there always is the necessity to find a suitable compromise between the length of the volume element and the intensity of the beam at a certain diffraction angle 2θ . Usually a diffraction angle 2θ between 4° and 10° is used. Therefore, in case of components, due the transmission geometry large beam path lengths occur (fig. 4). This as well as the shape of the volume element

The half width of the reflections increases with increasing energy value and decreasing Bragg angle θ . The width of the reflection itself is not a measure for the quality of the determination of the line position in residual stress analyses, but it becomes important in those cases where an overlapping of reflections occurs [13], e.g. in case of multiphase materials or structures that are not highly symmetric and of high energy values which are equivalent to low d-spacings and thus a high reflection density.

With respect to a reduction of the reflection overlapping, a smaller 2θ angle can be used. This, of course, also has the consequence of a comparably higher reflection intensity but also a larger gauge volume as discussed before.

6. Implications of the material investigated: Coarse grains and texture

In case of coarse grained materials instead of the usual smooth curve an overlapping of several curves is visible. Since the single grains contributing to the curve are situated at different positions within the gauge volume, the reflections arise from positions that usually are off-center and the line positions therefore are shifted. This shift superimposes on the line position shift induced by the residual stresses. Usually both effects cannot be separated. Thus, in case of coarse grained materials either a single crystal measurement and evaluation technique [14] or an oscillation of the sample e.

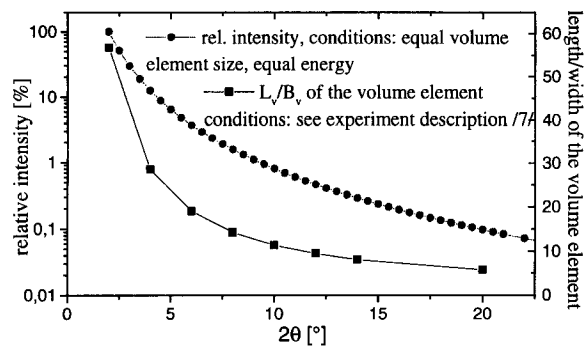


Fig. 3: Dependence of gauge volume size and relative intensity of the reflections on the diffraction angle 2θ

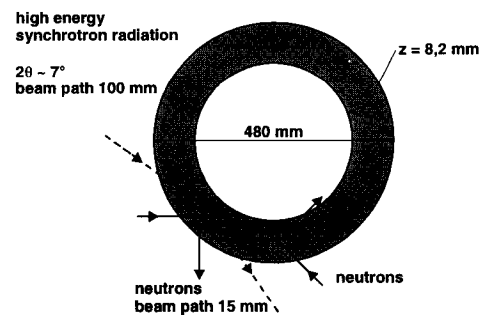


Fig. 4: Beam path lengths in components

g. in the inclination angle ψ is necessary. The grain size d_c above which the material has to be classified as coarse grained can be estimated using the image that the Debye-Scherrer ring should be completely occupied:

$$d_c = \frac{360^\circ \cdot 360^\circ}{J \cdot \Delta\theta_0 \cdot ms}$$

The fat dot symbolises a convolution between the beam divergence $\Delta\theta_0$ and the mosaic spread ms of the crystals. In case of synchrotron diffraction, due to the small beam divergence this convolution roughly can be substituted by the mosaic spread alone. The critical grain size decreases with decreasing gauge volume and decreasing mosaic spread of the crystals and multiplicity factor.

Besides the grain size texture is an implication of the material that has a major effect on the spectra. The small volume element achievable in high energy synchrotron diffraction enables texture analysis with a high local resolution in the bulk of components. Thus, often a simultaneous analysis of the texture and the residual stresses can be performed.

7. Applications

An example where residual stress analyses was only feasible by using high energy synchrotron radiation is shown in fig. 5.

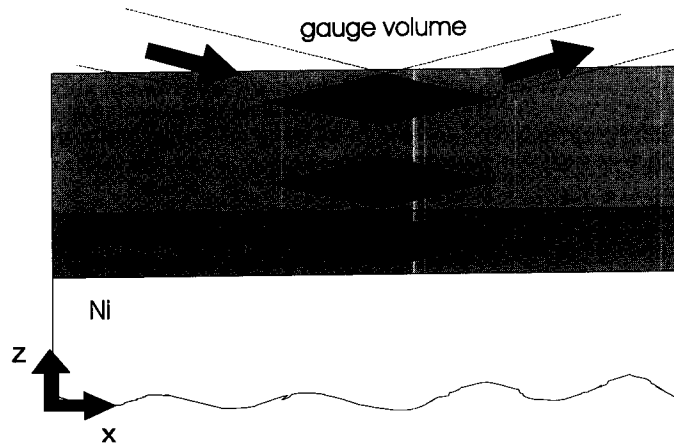


Fig. 5: Sample with indicated gauge volume positions

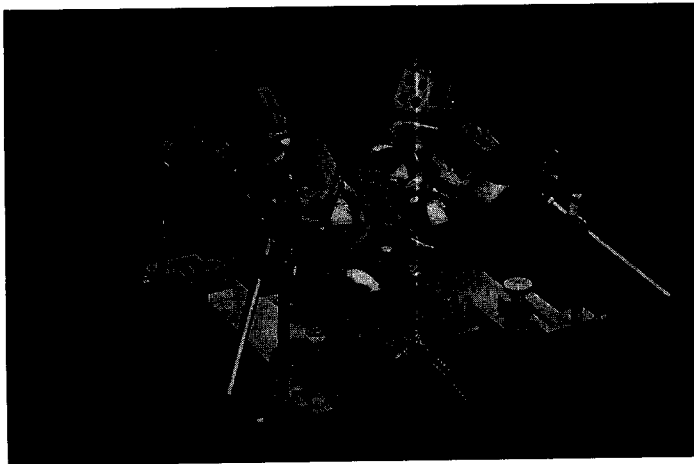


Fig. 6: Gradient oven device

A thermal barrier coating consists of a substrate, a bond coat and an adhesive layer in-between them. Thus, the residual stress distribution in the adhesive layer is not accessible using X-ray diffraction. The small thickness of the layer of approximately $100\mu\text{m}$ renders it impossible to determine the residual stresses by neutron diffraction. In case of high energy synchrotron radiation the volume element is so small that it fits into the layer (fig. 5). Furtheron, the high intensity of the beam allows for residual stress analyses in-situ under realistic thermal loading where in special furnace [15] the sample is heated from the top and cooled on the bottom (fig. 6). The result of the experiments show that while at 270K the in-plane residual stress σ_x in the bond layer is compressive with a value of -90 MPa, the stress σ_x in the bond layer decreases to app. -70 MPa at 770K and to app. -40 MPa at 1070K [15].

Simultaneous residual stress and texture analyses were performed on a cold extruded steel sample (German steel grade C15) of 15mm diameter.

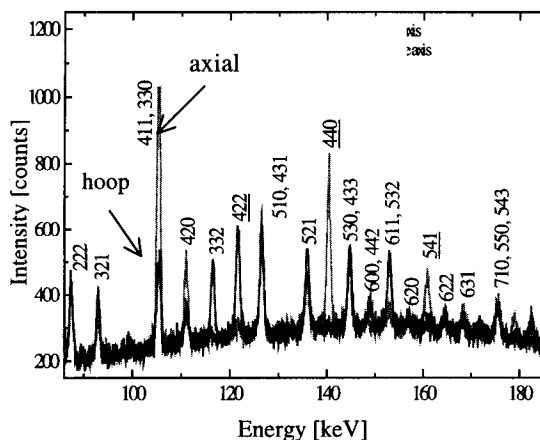


Fig. 7: Spectra in axial direction (light gray) and hoop direction of the extrudate

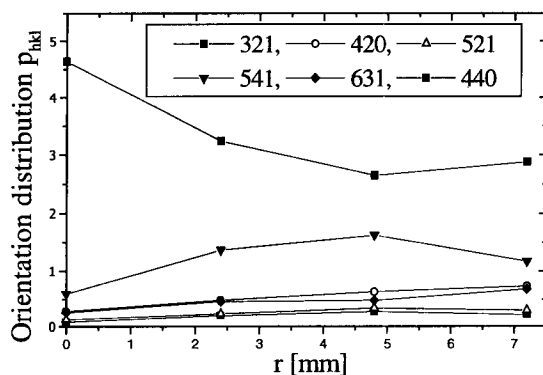


Fig. 8: Texture distribution across the sample diameter

longer than wide. The 2θ value chosen has to be a compromise between the decrease of the resolution and the decrease of the volume element's length with increasing 2θ value. The exact dimensions of the volume element apart from the angle 2θ also are determined by the width of the primary and the secondary slit.

The low divergence of the beam combined with the usually small volume element chosen in residual stress analyses with synchrotron radiation might result in coarse grain effects at significantly smaller grain sizes than it is the case in neutron diffraction.

The use of white radiation apart from giving access to high energy values also allows for a simultaneous investigation of residual stresses and texture.

8. Acknowledgements

The authors are grateful for the allocation of beam time at the beamline ID15A of the ESRF Grenoble, France.

The spectra in hoop and in axial direction of the sample (fig. 7) reveal the typical $\langle 110 \rangle$ -fibre texture typical for extruded bcc materials. A more detailed analysis of the texture strength variation across the sample diameter was performed using the axial spectra obtained at different positions across the sample diameter using the method presented in [4] (fig. 8). Obviously the texture is the most pronounced in the centre of the sample, which is a consequence of the well-known material flow pattern in extrusion, where the core is faster deformed than the surface, which is due to friction between the extrudate and the die [16].

8. Summary and Conclusions

High energy synchrotron diffraction recently has been introduced as a new method for residual stress analyses. Due to the high intensity of the synchrotron beam, the large spectral range and high energy values available at modern synchrotron sources, penetration depths comparable to those of neutrons often can be reached at significantly shorter measuring times and in significantly smaller gauge volumes. Although the resolution of energy dispersive measurements is significantly lower than in case of angle dispersive analyses, the determination of the line position and thus the residual stress can be done with an accuracy almost comparable to neutron diffraction. Since the intensity of the reflections strongly decreases with increasing Bragg angle θ measurements have to be performed at low 2θ values. Thus, the volume element has the shape of an elongated diamond that is significantly

9. References

- [1] A. J. Allen, C. Andreani, M. T. Hutchings and C. G. Windsor, *NDT International*, pp. 249-254 (1981).
- [2] H. F. Poulsen and D. J. Jensen, in *Proc. 16th Risø International Symposium on Materials Science*, N. Hansen, D. J. Jensen, Y. L. Liu and B. Ralph, eds., (1995).
- [3] J. Bordas, I. H. Munro and A. M. Glazer, *Nature*. 262: 541-545 (1976).
- [4] L. Gerward, S. Lehn and G. Christiansen, *Texture of Crystalline Solids 2*: 95-111 (1976).
- [5] T. A. Kuntz, H. N. G. Wadley and D. R. Black, Review of Progress in *Quantitative Non-destructive Evaluation*, 11: 331-338 (1992).
- /6/ H. Ruppertsberg, *Adv. X-ray Analysis*. 37: 235-244 (1994).
- /7/ W. Reimers, A. Pyzalla, M. Broda, G. Brusch, D. Dantz, K.-D. Liss, T. Schmackers and T. Tschentscher, *J. Mat. Sci. Letters*. 18: 581-583 (1999).
- /8/ K.-D. Liss, A. Royer, T. Tschentscher, P. Suortti and A. P. Williams, *J. Synchrotron Rad.* 5: 82-89 (1998).
- /9/ B. Dziunikowski, in *Energy Dispersive X-ray Fluorescence Analysis, Comprehensive Analytical Chemistry*, G. Svehla ed., (Elsevier, Amsterdam 1989).
- /10/ P. J. Webster, X. D. Wang and G. Mills, in *Proc. ECRS 4*, S. Denis, J.-L. Lebrun, N. Bourmiquel, M. Barral and J.-F. Flavenot, eds., (June 4-6 1996, Cluny, France), pp. 127-134.
- /11/ G. Brusch, in *Entwicklung eines Meß-und Auswerteverfahrens zur Analyse von Eigenspannungen mit Hochenergie-Röntgenbeugung*, Berichte aus dem Zentrum für Eigenspannungsanalyse, W. Reimers, ed., (Hahn-Meitner-Institut Berlin, 1998).
- /12/ E. Pluyette, J. M. Sprauel, A. Lodini, M. Perrin and P. Todeschini, in *Proc. ECRS 4*, S. Denis, J.-L. Lebrun, N. Bourmiquel, M. Barral and J.-F. Flavenot, eds., (June 4-6 1996, Cluny, France), pp. 153-163.
- /13/ C. G. Windsor, in *Measurement of Residual and Applied Stress Using Neutron Diffraction*, M. T. Hutchings and A. Krawitz, eds., NATO ASI Series E, Vol. 216, pp. 285-296.
- /14/ W. Reimers, in *Measurement of Residual and Applied Stress Using Neutron Diffraction*, M. T. Hutchings and A. Krawitz, eds., (Kluwer Academic Publishers, 1992), pp. 159-170.
- /15/ T. Schmackers, W. Reimers, H.U. Baron, T. Cosack, in: *Proc. of Materials for Advanced Power Engineering*, 1647 - 1656, 5.-7.10.1998, Liège, J. Lecomte-Beckers, F. Schubert, P.J. Ennis (ed.), III, (1998)
- /16/ A.Pyzalla, W.Reimers, A.Royer, K.-D.Liss, *Proc. 20th Risoe International Symposium on Materials Science: Deformation-Induced Microstructures: Analysis and Relation to Properties*. Editors: J.B.Bilde-Soerensen, J.V.Carstensen, N.Hansen. D. Juul Jensen, T.Leffers, W.Pantleon, O.B.Pedersen, G.Winther, Risoe National Laboratory, Roskilde, Denmark 1999, pp. 453 - 458